MOTORSPORTS

A Single-Element Multi-Point Compliance for Rigid-Body Connections

Behzad Danaei*, Srikanth Sivaramakrishnan
General Motors

* Behzad Danaei is currently with Zoox.

MOTORSPORTS

Motivation

Problem: Two Bodies Connected at Multiple Mounts

Many assemblies connect two rigid bodies at multiple mounting points through compliant elements.

1. **Common in vehicles**

   Subframe-to-chassis interfaces, engine mounts, exhaust hangers, double-wishbone control arms with front/rear bushings.

2. **Each mount is a 6-DOF compliance**

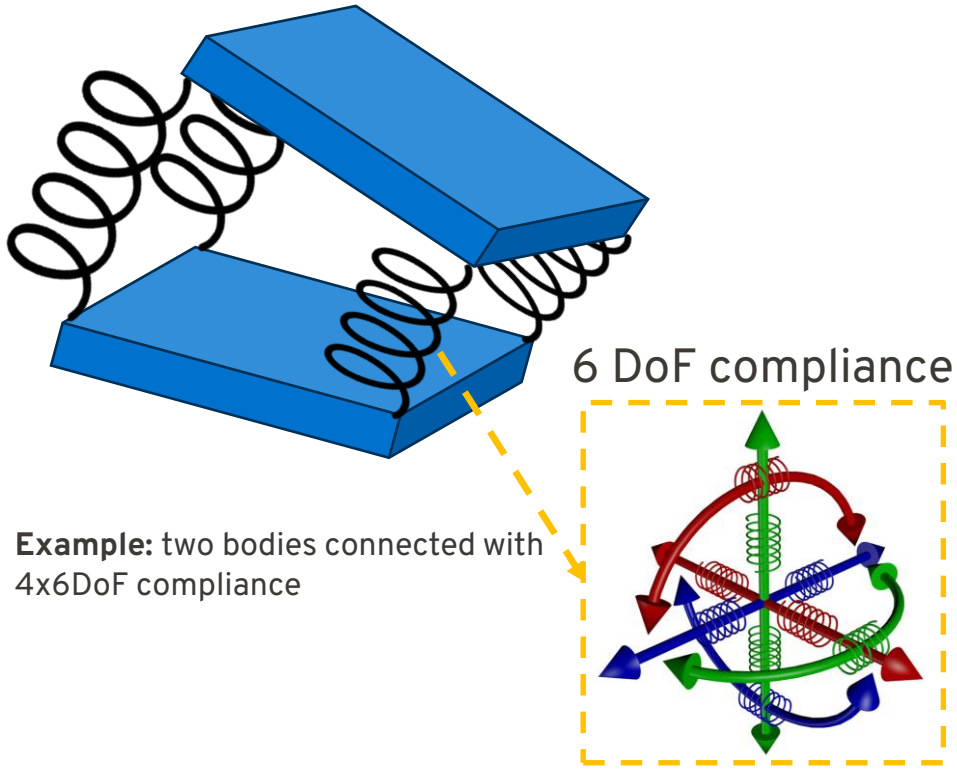
   Deforms in three translational and three rotational directions; stiffness may be anisotropic.

3. **High stiffness**

   Benchmark mounts: ~10^7 N/m each, ~10^8 N/m in aggregate, representative of production isolation mounts.

4. **Offline and real-time use**

   The model should suit both offline and real-time / HIL simulation.



Example: two bodies connected with 4x6DoF compliance

Gap: no existing element aggregates an arbitrary set of mounts into one well-conditioned compliance

Spatial stiffness theory and 6-DOF bushing models are well established; this aggregation is not.

Conventional approach: 6-DOF Compliance per Mount

Conceptually straightforward: each element maps relative displacement to force and moment.

DRAWBACK 1 · INSTABILITY

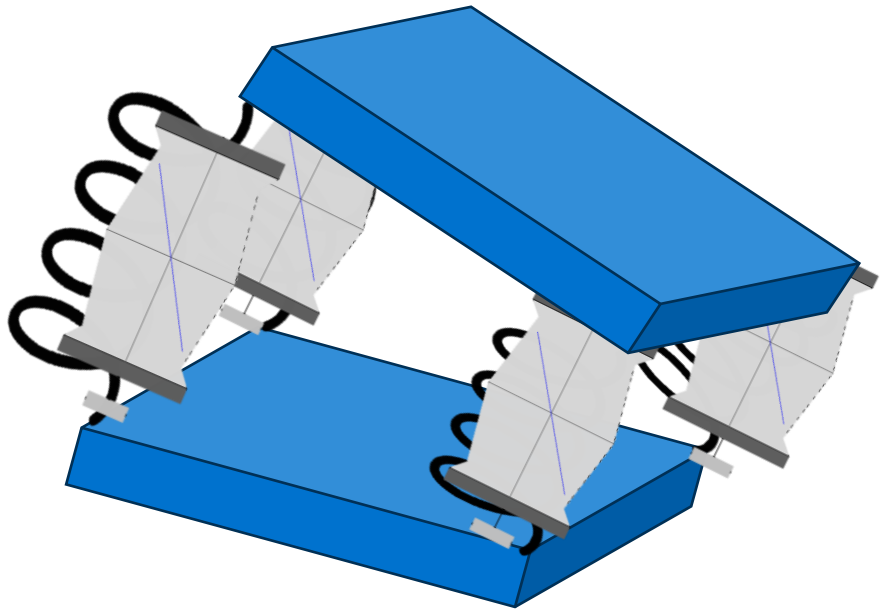
Small stable step size

- Aggregate stiffness drives natural frequencies into the kHz range
- Explicit Euler needs sub-microsecond steps

DRAWBACK 2 · COST AND NUMERICS

Cost grows with n

- Each compliance element adds 12 variables to the system
- Kinematic loops, extra algebraic states, brittle numerics



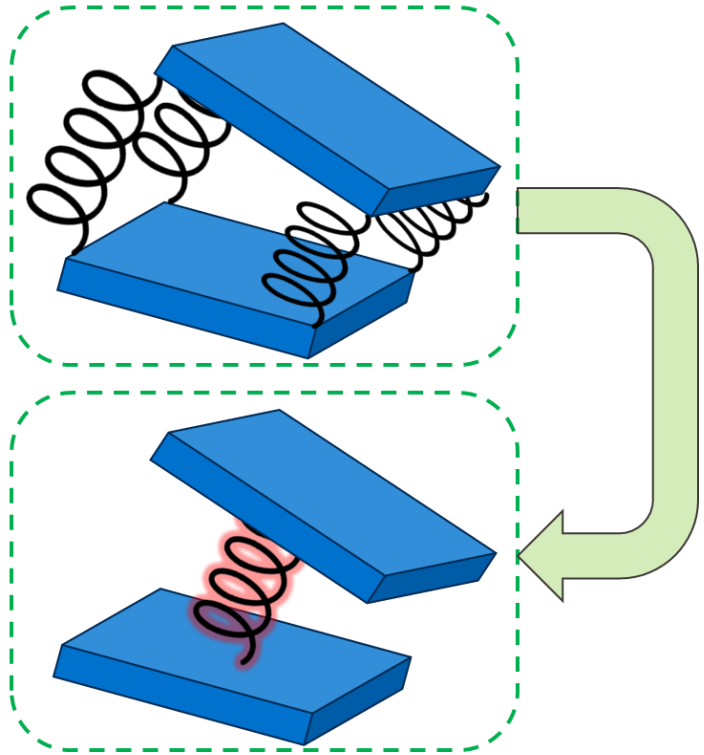
Benchmark (n = 10): stable only at $h = 10^{-7}$ s, about 40× slower than real time

Proposed: Single-Element Multi-Point Compliance (SEMPC)

MOTORSPORTS

One element, functionally equivalent to the combined effect of n individual 6-DOF compliances.

- **Equivalent to the n mounts** to first order in relative orientation
- **6×6 spatial stiffness** precomputed from mount geometry and local stiffnesses
- **No extra algebraic unknowns or kinematic loops** compared with an ordinary bushing
- **Linear map** distributes the net wrench back to each mount
- **Second-order filter** for stability at high stiffness and real-time step sizes



n mounts → one precomputed 6×6 matrix

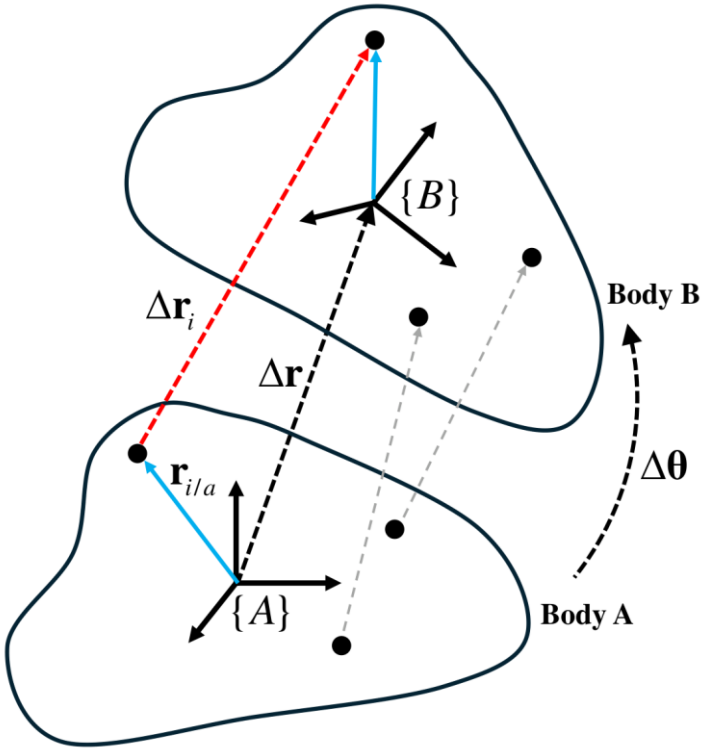
Runtime dynamics: one 6-DOF element with a fixed number of states, regardless of n.

MOTORSPORTS

SEMPC Formulation

Kinematics: Displacement at Each Mount

Relative motion of {B} with respect to {A}, linearized for small relative rotations.



$$\Delta \mathbf{r}_i = \Delta \mathbf{r} - \left[\mathbf{r}_{i/a}\right]_\times \Delta \boldsymbol{\theta}$$

$$[\mathbf{a}]_\times = \begin{bmatrix} 0 & -a_z & a_y \\ a_z & 0 & -a_x \\ -a_y & a_x & 0 \end{bmatrix}, \qquad [\mathbf{a}]_\times \mathbf{b} = \mathbf{a} \times \mathbf{b}$$

- $\Delta\mathbf{r}$, $\Delta\boldsymbol{\theta}$: relative translation and small rotation of {B}, resolved in {A}
- $\mathbf{r}_{i/a}$: vector from the origin of {A} to mount i
- **First order on SO(3)**: truncation error $O(|\Delta\theta|^2)$, valid for typical mount deflections

Each mount deflection Δr_i is linear in the same six coordinates (Δr, $\Delta\theta$)

Local Mount Laws and the Net Wrench

Each mount is a linear spring; the n mounts act in parallel between bodies A and B.

LOCAL LAW AT MOUNT i

$$\mathbf{F}_i = \mathbf{K}_i \, \Delta\mathbf{r}_i, \qquad \mathbf{M}_i = \mathbf{K}_{\theta,i} \, \Delta\boldsymbol{\theta}$$

NET WRENCH AT {A}

$$\mathbf{F} = \sum_{i=1}^{n} \mathbf{F}_i, \qquad \mathbf{M} = \sum_{i=1}^{n} \left(\mathbf{M}_i + \mathbf{r}_{i/a} \times \mathbf{F}_i \right)$$

- $\mathbf{K}_i, \mathbf{K}_{\theta,i} \in \mathbb{R}^{3\times3}$: translational and rotational stiffness of mount i (possibly anisotropic)
- All mount deflections depend on the same ($\Delta\mathbf{r}, \Delta\boldsymbol{\theta}$)
- $\mathbf{r}_{i/a} \times \mathbf{F}_i$: moment of each mount force about {A}

Substituting the kinematics into the local laws gives one linear map from pose to wrench

Central Result: Aggregate 6×6 Spatial Stiffness

To first order, the mount assembly is equivalent to a single 6-DOF element.

$$\begin{bmatrix} \mathbf{F} \\ \mathbf{M} \end{bmatrix} = \mathcal{K} \begin{bmatrix} \Delta\mathbf{r} \\ \Delta\boldsymbol{\theta} \end{bmatrix} \qquad \mathcal{K} = \sum_{i=1}^{n} \begin{bmatrix} \mathbf{K}_i & -\mathbf{K}_i[\mathbf{r}_{i/a}]_\times \\ [\mathbf{r}_{i/a}]_\times \mathbf{K}_i & \mathbf{K}_{\theta,i} - [\mathbf{r}_{i/a}]_\times \mathbf{K}_i [\mathbf{r}_{i/a}]_\times \end{bmatrix}$$

TRANSLATION

ΣK_i

- Sum of the translational stiffnesses

COUPLING

$\pm K_i[r_{i/a}]_\times$

- Translation–rotation coupling from the mount offsets

ROTATION

$K_{\theta,i} - [r]_\times K_i [r]_\times$

- Rotational stiffness plus the contribution of translational stiffness at an offset

$\mathcal{K}$ depends only on geometry and local stiffnesses: precomputed before simulation

Assembled and inverted once; no matrix factorization at runtime.

Per-Mount Wrench Distribution (Load Splitter)

The solver needs only the net wrench; per-mount loads are useful for sensing and diagnostics.

$$\begin{bmatrix}\mathbf{F}\\ \mathbf{M}\end{bmatrix} \xrightarrow{\mathcal{K}^{-1}} \begin{bmatrix}\Delta\mathbf{r}\\ \Delta\boldsymbol{\theta}\end{bmatrix} \xrightarrow{\mathcal{A}_i} \begin{bmatrix}\mathbf{F}_i\\ \mathbf{M}_i\end{bmatrix}$$

$$\mathcal{A}_i \triangleq \begin{bmatrix}\mathbf{K}_i & -\mathbf{K}_i[\mathbf{r}_{i/a}]_\times\\ \mathbf{0} & \mathbf{K}_{\theta,i}\end{bmatrix} \qquad \begin{bmatrix}\mathbf{F}_i\\ \mathbf{M}_i\end{bmatrix} = \underbrace{\mathcal{A}_i\,\mathcal{K}^{-1}}_{\text{precomputed } 6\times6} \begin{bmatrix}\mathbf{F}\\ \mathbf{M}\end{bmatrix}$$

- $\mathcal{K}^{-1}$: net wrench → relative pose; $\mathcal{A}_i$: relative pose → wrench at mount i
- $\mathcal{K}^{-1}$ and $\mathcal{A}_i$ are precomputed parameters: one matrix–vector product per mount at runtime
- Load splitter consistent with the assumed local stiffnesses

Per-mount loads with no additional states and no change to the step size

Dynamic Extension: Second-Order Filter in Wrench Space

For very stiff $\mathcal{K}$ at larger steps: apparent inertia and viscous damping in compliance coordinates.

$$\mathcal{K}^{-1}\begin{bmatrix}\mathbf{F}\\ \mathbf{M}\end{bmatrix} = \tau^2\frac{d}{dt}\begin{bmatrix}\mathbf{v}_{\text{rel}}\\ \boldsymbol{\omega}_{\text{rel}}\end{bmatrix} + 2\zeta\tau\begin{bmatrix}\mathbf{v}_{\text{rel}}\\ \boldsymbol{\omega}_{\text{rel}}\end{bmatrix} + \begin{bmatrix}\Delta\mathbf{r}\\ \Delta\boldsymbol{\theta}\end{bmatrix}$$

$$\underbrace{\tau^2\ddot{\boldsymbol{\delta}}}_{\text{inertance}} + \underbrace{2\zeta\tau\dot{\boldsymbol{\delta}}}_{\text{damper}} + \underbrace{\boldsymbol{\delta}}_{\text{spring}} = \mathbf{u} = \mathcal{K}^{-1}\begin{bmatrix}\mathbf{F}\\ \mathbf{M}\end{bmatrix}, \qquad \tau = \frac{1}{2\pi f_c}$$

- At steady state $\boldsymbol{\delta} = \mathbf{u} = \mathcal{K}^{-1}[\mathbf{F}; \mathbf{M}]$, the static compliance
- Lowers the natural frequency: highest active frequency limited to $\mathbf{f}_c$
- Applied separately to the translational and rotational channels
- Fixed **12-state** runtime ODE (Δr, $\Delta \dot{r}$, $\Delta\theta$, $\Delta\theta$), for any n

Explicit state form: avoids algebraic loops and stays robust at high stiffness

Choosing the Filter Time Constant τ

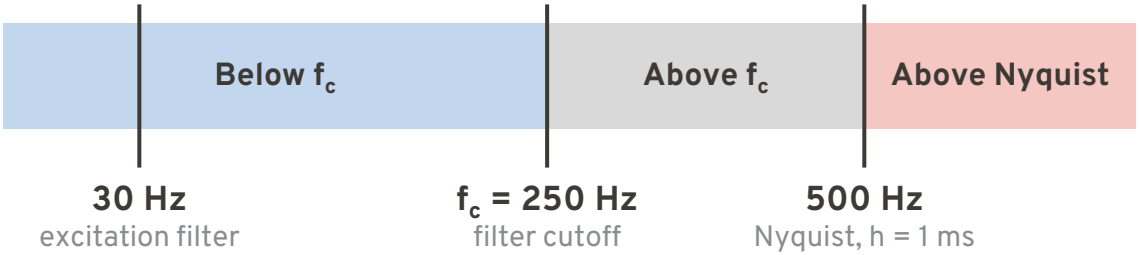
Compliance natural frequency: above the highest excitation to preserve, below the Nyquist limit of the step.

STABILITY BOUND, EXPLICIT EULER WITH STEP h

$$\tau > \begin{cases} \dfrac{h}{2\zeta}, & 0 < \zeta \leq 1 \\ \dfrac{h}{2}\left(\zeta + \sqrt{\zeta^2 - 1}\right), & \zeta > 1 \end{cases}$$

with $\tau = 1/(2\pi f_c)$

BENCHMARK VALUES



- **Lower limit on f_c:** highest excitation frequency that must be preserved
- **Upper limit on f_c:** Nyquist limit of the integration step

Accuracy–efficiency trade-off: a small filter error in exchange for a $10^4\times$ larger step

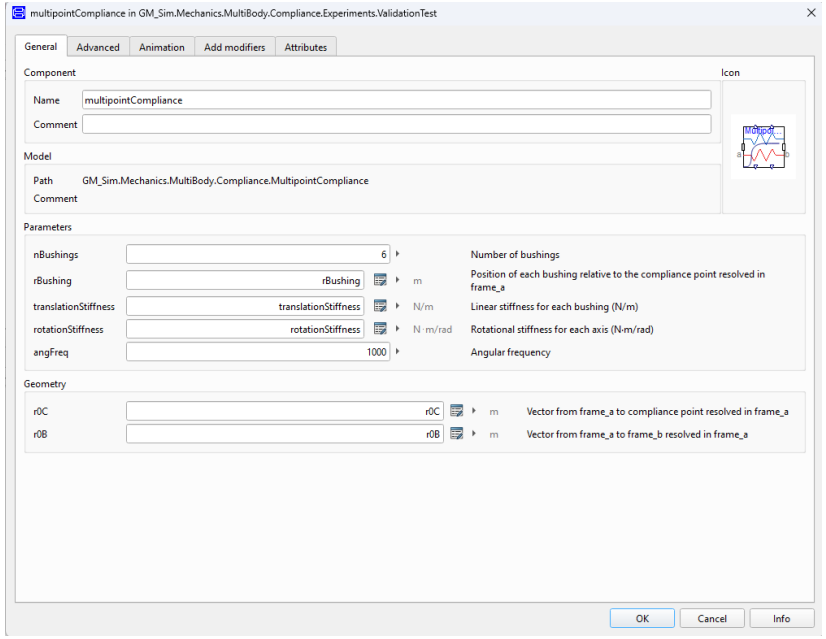
Benchmark: excitation filtered at 30 Hz, f_c = 250 Hz, h = 1 ms.

MOTORSPORTS

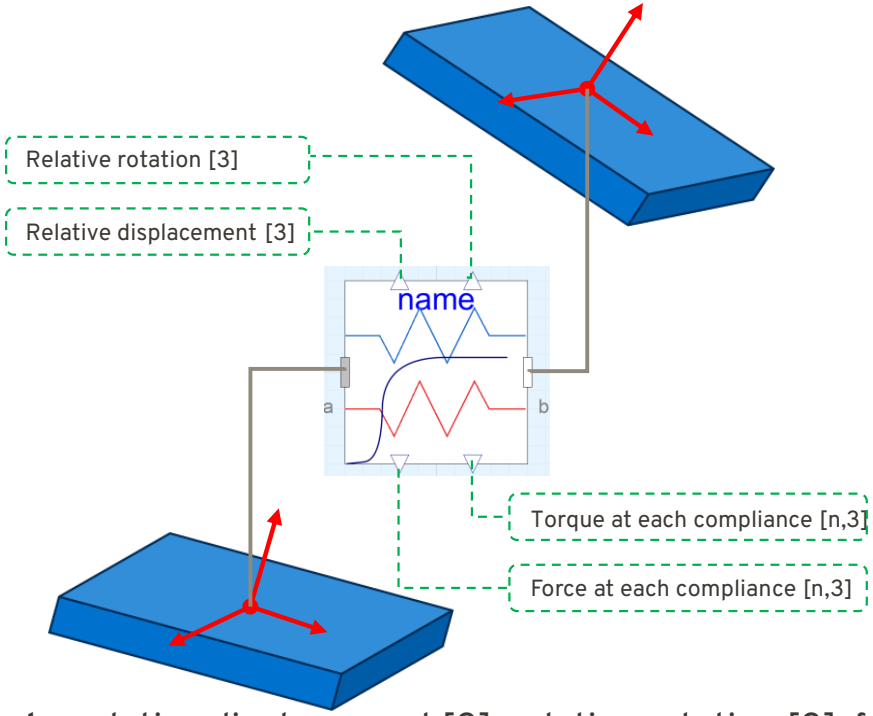
Modelica Implementation

MultiMount Component: Parameters and Outputs

A Modelica component with MultiBody frame_a and frame_b connectors.



- **Parameters**: number of bushings; location, translational and rotational stiffness of each bush [n,3]; filter frequency and damping ratio

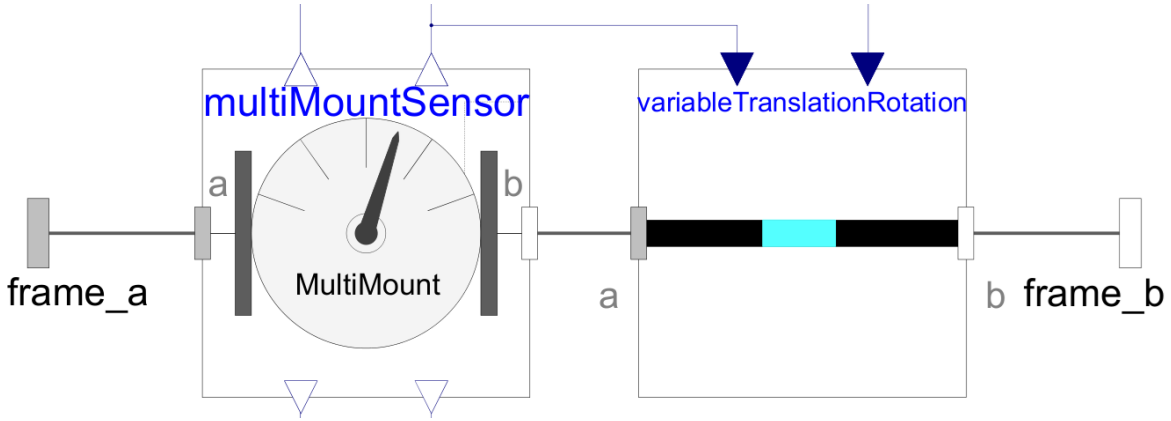


- **Outputs**: relative displacement [3], relative rotation [3], force and torque at each mount [n,3]

The runtime ODE has 12 states for any number of mounts

Inside the Component: Sensor + Filtered Actuator

Two cooperating sub-models between frame_a and frame_b.



SUB-MODEL 1 · MultiMountSensor

Passive, zero-displacement observer

- Reads [**F**; **M**] at frame_a; outputs [Δ**r**; Δ**θ**] = $\mathcal{K}^{-1}$[**F**; **M**] and per-mount loads
- frame_a and frame_b connected directly: **no dynamic states**

SUB-MODEL 2 · VariableTranslationRotation

Second-order filter actuator

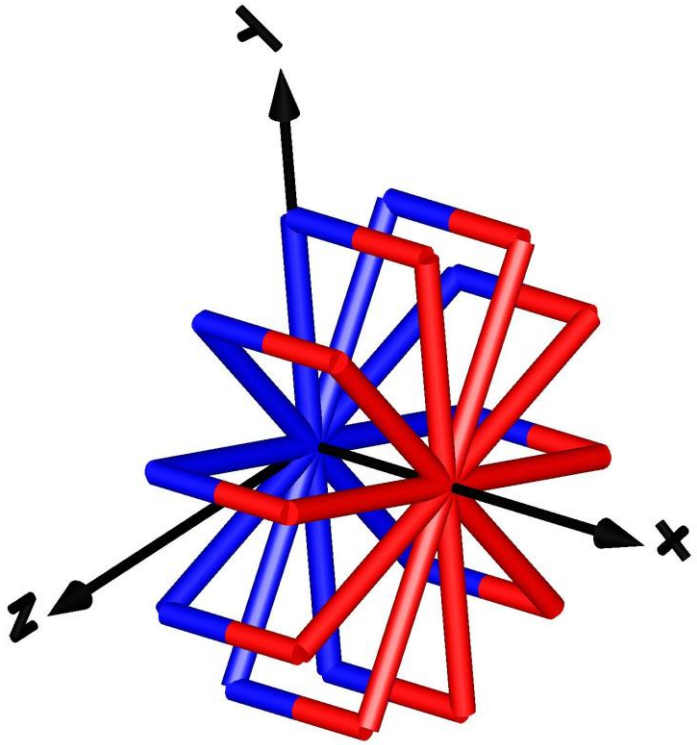
- Takes (Δ**r**, Δ**θ**) as target and integrates $\tau^2\ddot{\delta} + 2\zeta\tau\dot{\delta} + \delta = u$
- Sets the filtered pose of frame_b; ODE states selected as simulation states

MOTORSPORTS

Results

Benchmark Setup

Same problem, two models: n independent 6-DOF linear spring-dampers (reference) vs. one SEMPC.



Item	Value
Bodies	Body A fixed; body B: m = 100 kg, I = 1 kg m^2, gravity off
Mount layout	n points on a circle, R = 0.3 m (y–z plane)
Stiffness scaling	$\mathbf{K}_i = \mathbf{K}_1(1+\alpha)^{i-1}$, α = 0.10 (same for $\mathbf{K}_{\theta,i}$)
$\mathbf{K}_1$	diag(2.27, 1.41, 2.17) × 10^7 N/m
$\mathbf{K}_{\theta,1}$	diag(2.87, 1.73, 0.84) × 10^5 N m/rad
Excitation on B	Noise → 30 Hz Butterworth; F: [70, 12, 44] kN, M: [1, 2, 4] kN m
Solver	Dymola, explicit Euler, fixed step, 0.5 s

Fixed-step explicit Euler, so the stability limits can be characterized precisely

Study 1: Numerical Stability and Real-Time Feasibility

n = 10 mounts, stiffness representative of production mounts: largest stable step for explicit Euler.

	Reference	SEMPC
Max. stable step h	1×10^{-7} s	1×10^{-3} s
Steps per simulated second	10^{7}	10^{3}
Wall-clock vs. real time	≈ 40× slower	≈ 25× faster
Highest active frequency	kHz range	250 Hz (f_c)

10^4×

larger stable step

≈ 25×

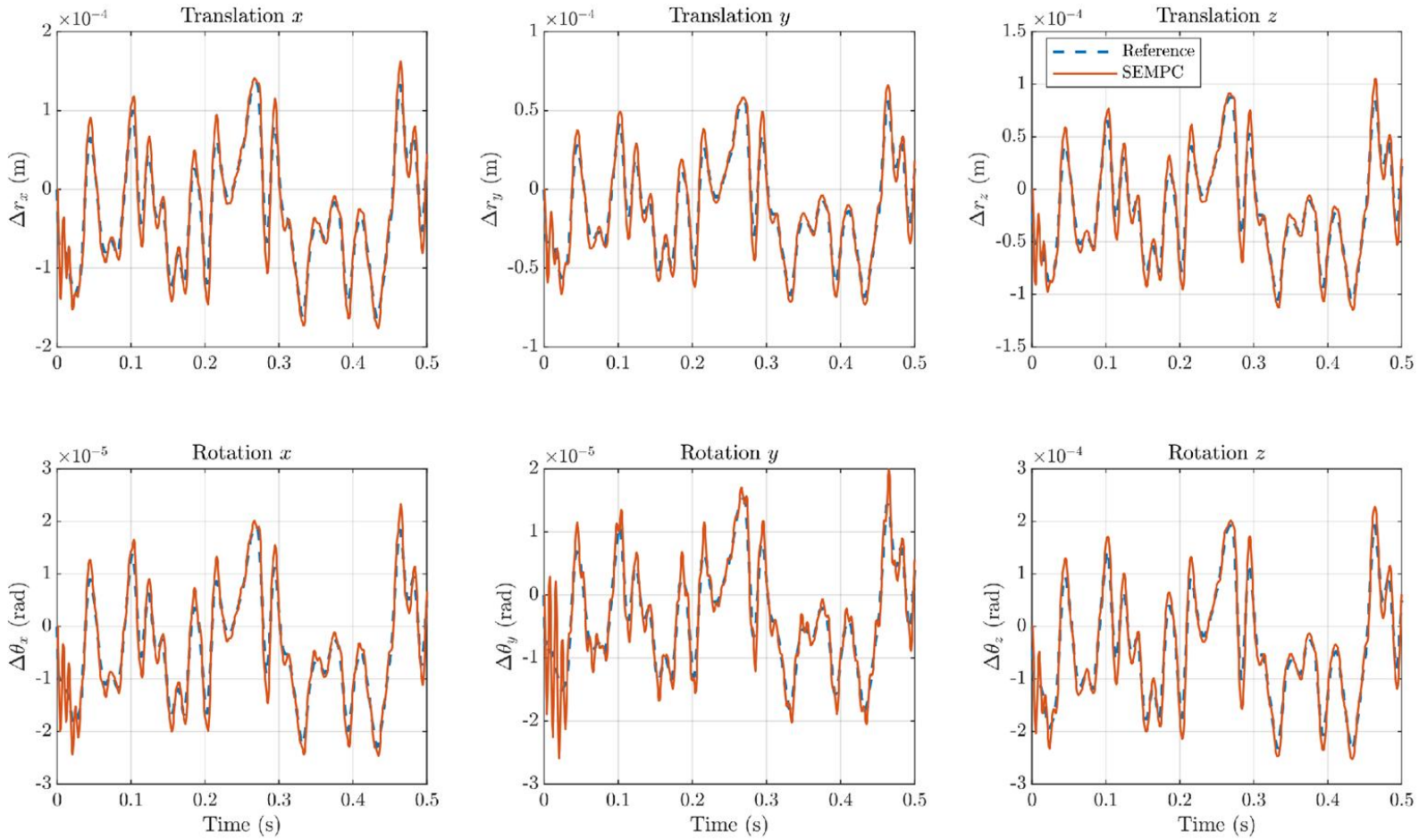
faster than real time

Real-time and hardware-in-the-loop (HIL) deployment within reach

The filter removes the direct coupling between stiff spring forces and the rigid-body equations.

Study 1: Relative Displacement of Body B

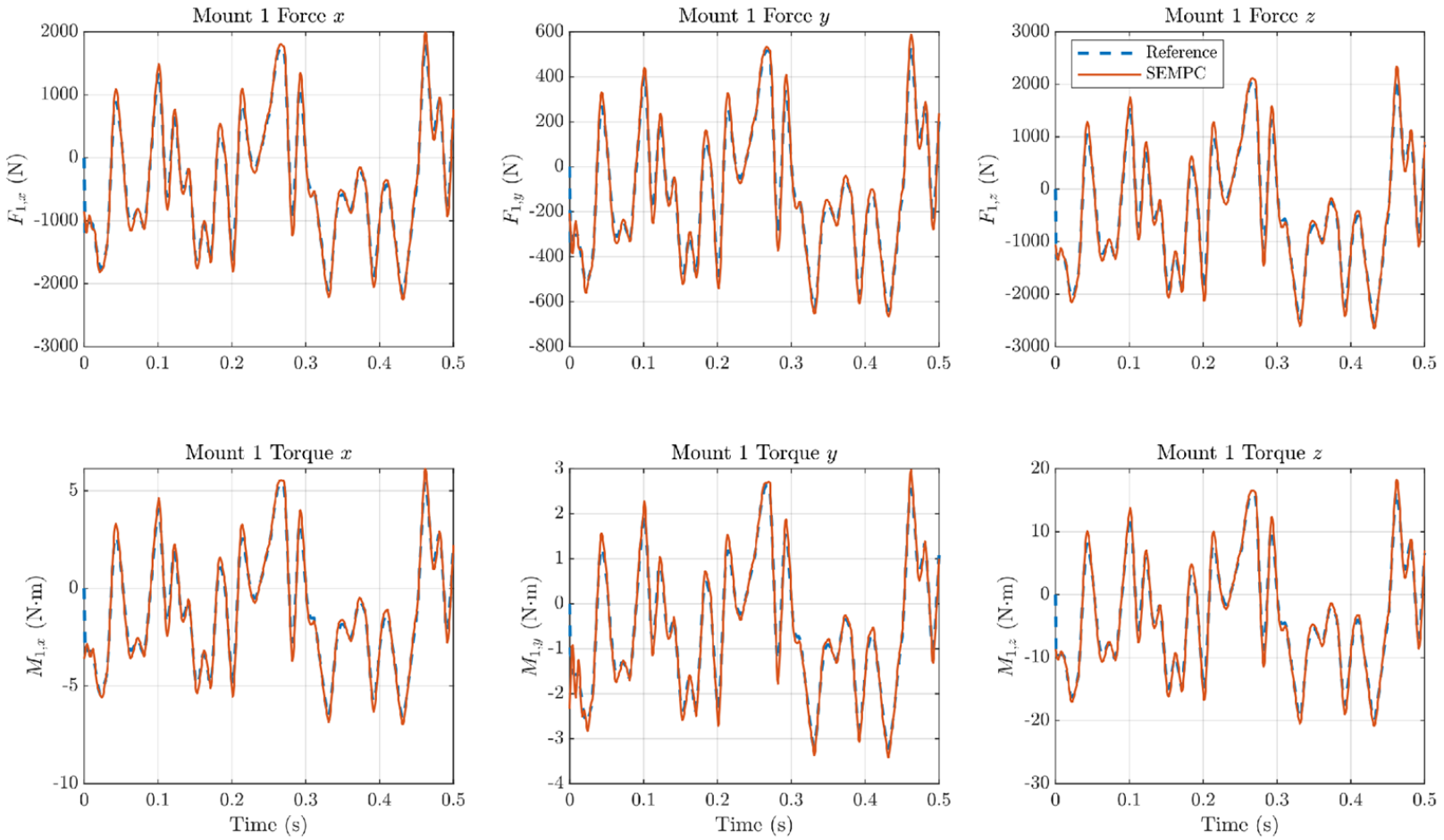
Relative translation (top) and rotation (bottom) of body B with respect to body A.



- **SEMPC** (solid orange) closely tracks the **reference** (dashed blue) across the dominant response modes
- The small error comes from the second-order filter: the **accuracy–efficiency trade-off**

Study 2: Per-Mount Load Recovery

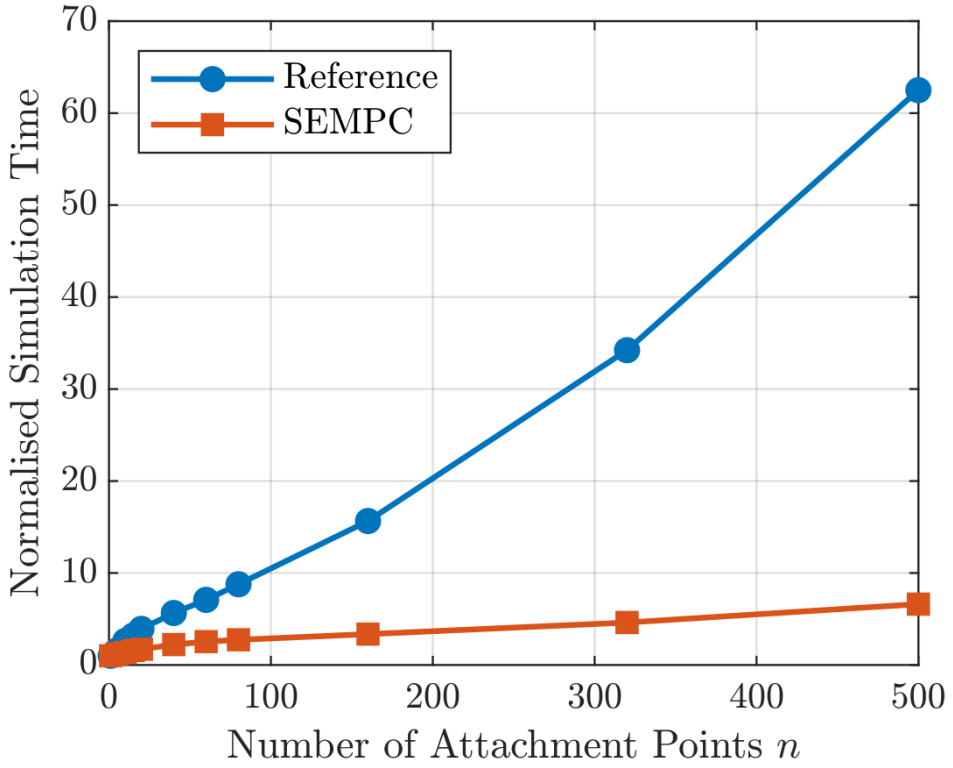
Force (top) and torque (bottom) at mount 1: load splitter vs. reference model.



- Load-splitter estimates agree closely with the reference across all attachment points
- **No additional differential states:** the sensor is an algebraic observer
- Can be used without the actuator: no impact on step size, model index or run time

Study 3: Computational Scalability

Normalised wall-clock time vs. number of attachment points n, all other parameters fixed.



REFERENCE

Cost increases clearly with n

- Each bushing adds elastic states; aggregate stiffness and natural frequencies grow with n

SEMPC

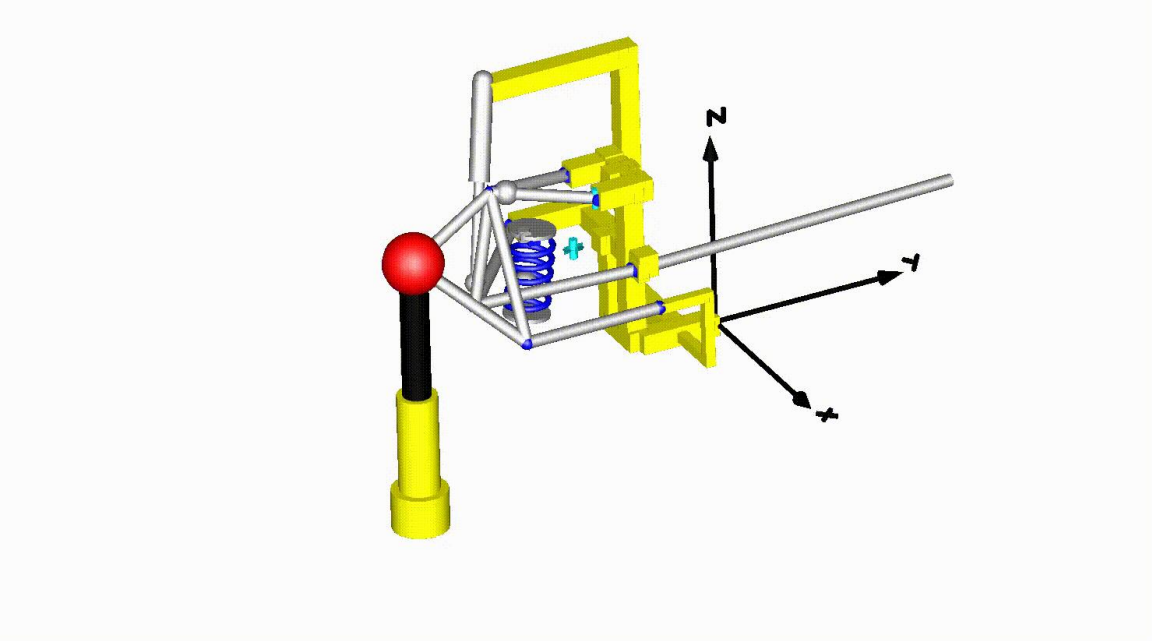
Much weaker growth with n

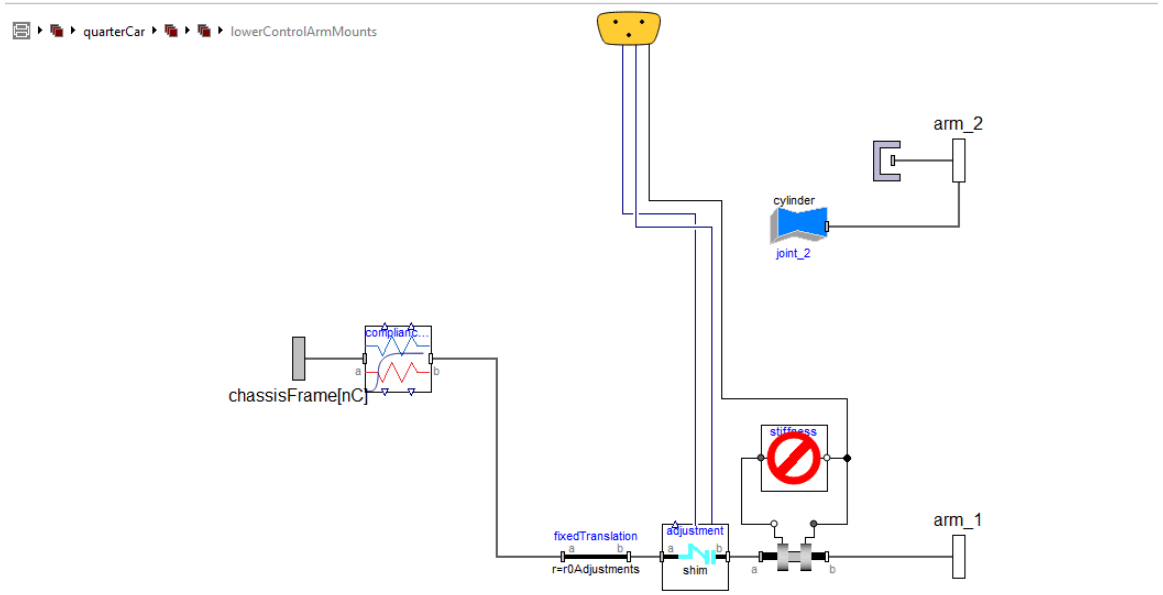
- n changes only the O(n) offline assembly; small increase from initialization and load splitting

Dimension reduction: for any number of mounts, one 6-DOF element with a fixed number of states

Application: Control Arm Mounts

Compliance added to the control arm mounts of a quarter-car model (lowerControlArmMounts).

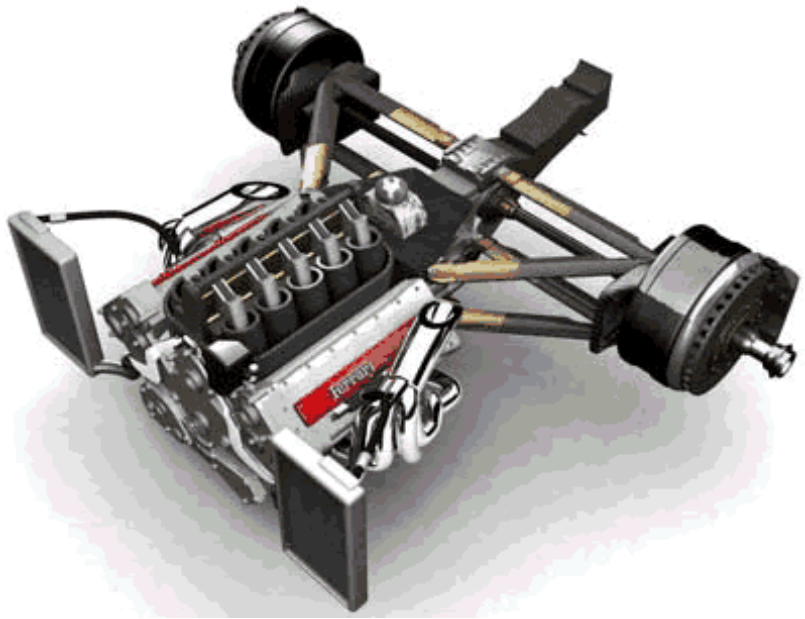


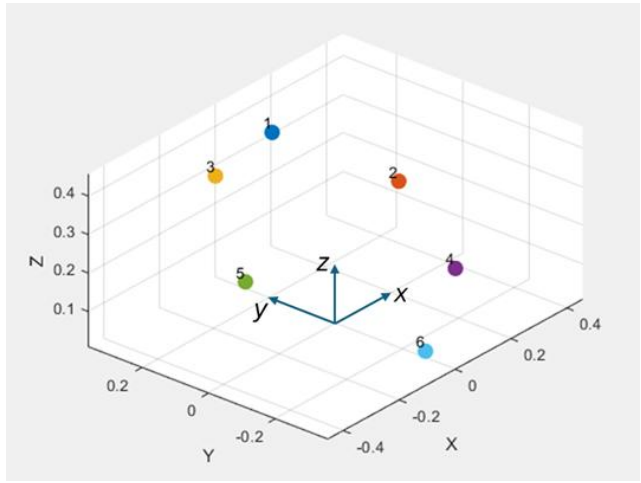


The force and moment at each mount are available, which was not possible directly before

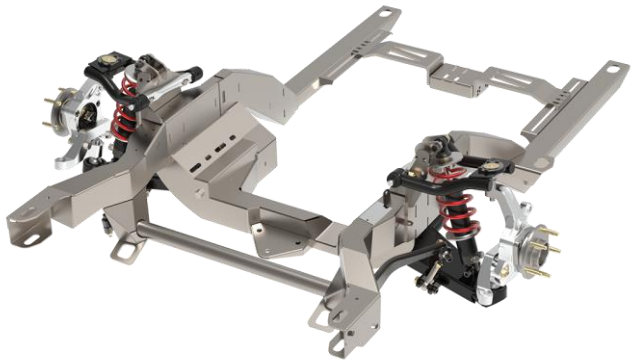
Applications: Engine–Chassis Interface and Subframes

Engine mounts and subframe-to-chassis interfaces are multi-mount connections.





Engine–chassis interface: engine and mount locations



Subframes

Limitations and Conclusions

MOTORSPORTS

Limitations

- First-order rotational approximation: reduced accuracy under **large relative rotations**
- Second-order filter introduces a small error versus the reference

Extensions

- Nonlinear or hysteretic mounts via incremental linearization: $\mathbf{K}_i(t)$, $\mathbf{K}_{\theta,i}(t)$ in the same assembly framework

Conclusions

- **One well-conditioned 6-DOF element** for a cluster of mounts
- **6×6 stiffness from geometry**, accurate to first order and precomputed
- **Per-mount load sensing** through a linear map, with no extra states
- **Second-order filter**: stable real-time performance at high stiffness (benchmark: 10^4× larger step)
- **Integrates into Modelica MultiBody models**

n mounts → one 6×6 matrix → 12-state runtime ODE


MOTORSPORTS

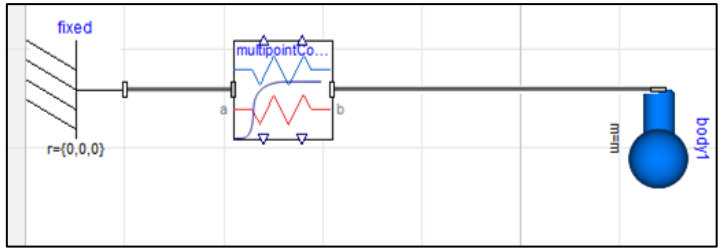
MOTORSPORTS

Backup

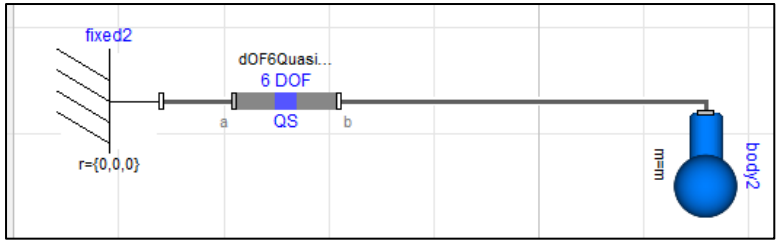
Backup: Computation Cost vs. Claytex QS and Dynamic 6-DOF

MOTORSPORTS

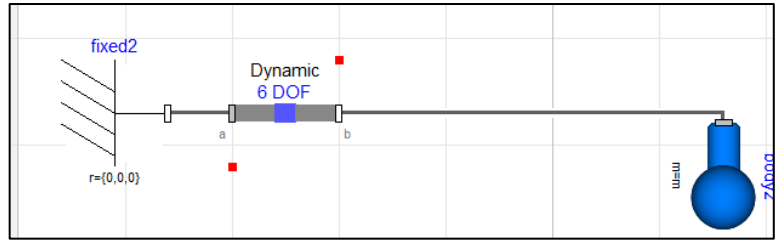
Additional results, not included in the paper. Fixed step 0.001 s, T = 1000 s.



Multi-mount 6 DoF QS



Claytex 6-DoF QS



Dynamic 6-DoF

```
Integration terminated successfully at T = 1000
   CPU-time for integration          : 0.472 seconds
   CPU-time for one grid interval    : 0.00472 milliseconds
   CPU-time for initialization       : 0 seconds
   Number of result points           : 100002
   Number of grid points             : 100001
   Number of accepted steps          : 1000000
   Number of f-evaluations (dynamics) : 1000000
   Number of Jacobian-evaluations    : 0
   Number of model time events       : 0
   Number of input time events       : 0
   Number of state events            : 0
   Number of step events             : 0
   Minimum integration stepsize      : 0.001
   Maximum integration stepsize      : 0.001
   Maximum integration order         : 1
Calling terminal section
... "dsfinal.txt" creating (final states)
```

```
Integration terminated successfully at T = 1000
   CPU-time for integration          : 2.93 seconds
   CPU-time for one grid interval    : 0.0293 milliseconds
   CPU-time for initialization       : 0 seconds
   Number of result points           : 100002
   Number of grid points             : 100001
   Number of accepted steps          : 1000000
   Number of f-evaluations (dynamics) : 1000000
   Number of Jacobian-evaluations    : 0
   Number of model time events       : 0
   Number of input time events       : 0
   Number of state events            : 0
   Number of step events             : 0
   Minimum integration stepsize      : 0.001
   Maximum integration stepsize      : 0.001
   Maximum integration order         : 1
Calling terminal section
... "dsfinal.txt" creating (final states)
```

```
Integration terminated successfully at T = 1000
   CPU-time for integration          : 3.13 seconds
   CPU-time for one grid interval    : 0.0313 milliseconds
   CPU-time for initialization       : 0.003 seconds
   Number of result points           : 100002
   Number of grid points             : 100001
   Number of accepted steps          : 1000000
   Number of f-evaluations (dynamics) : 1000000
   Number of Jacobian-evaluations    : 0
   Number of model time events       : 0
   Number of input time events       : 0
   Number of state events            : 0
   Number of step events             : 0
   Minimum integration stepsize      : 0.001
   Maximum integration stepsize      : 0.001
   Maximum integration order         : 1
Calling terminal section
... "dsfinal.txt" creating (final states)
```

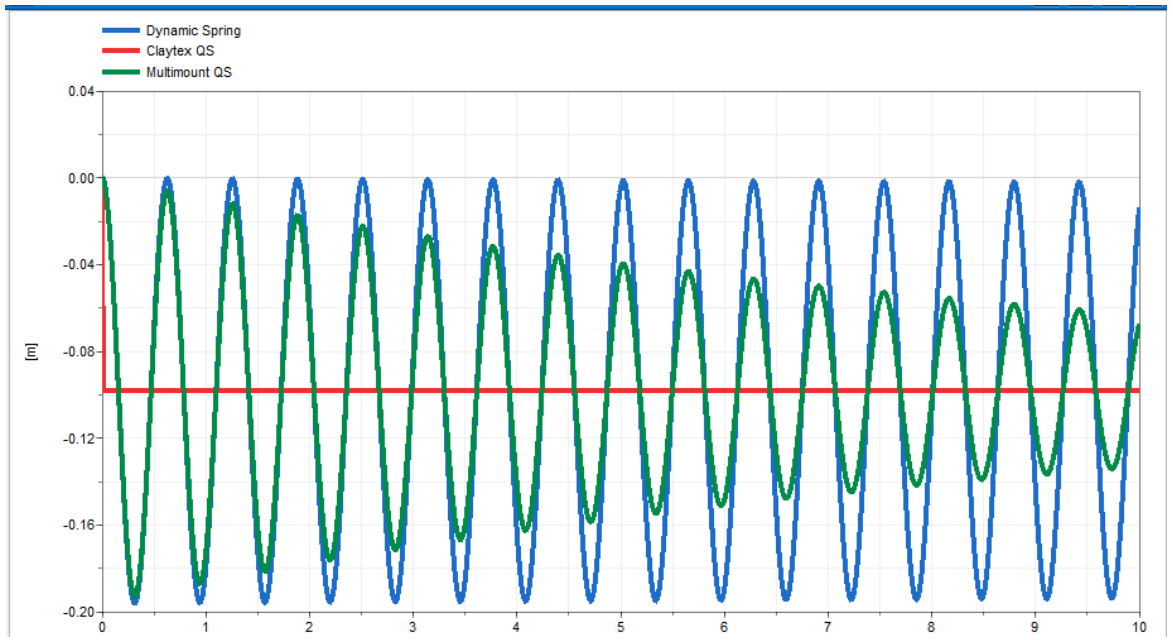
Multi-point 6-DOF QS: 6.2× faster than the Claytex 6-DOF QS, 6.6× faster than the dynamic bushing

CPU time for integration: 0.472 s (multi-point QS), 2.93 s (Claytex QS), 3.13 s (dynamic 6-DOF).

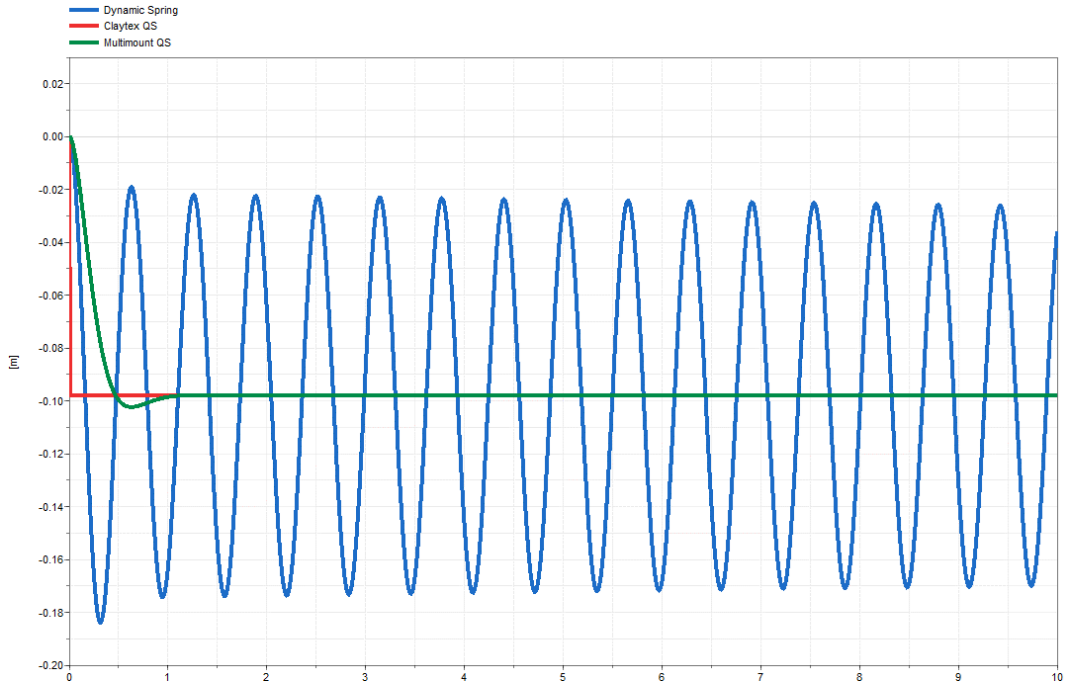
Backup: Transient Response vs. Claytex 6-DOF QS

Additional results, not included in the paper. 10 kg mass hanging from a 1000 N/m spring, no damping.

Angle Freq = 1000 Hz



Angle Freq = 50 Hz



Claytex QS shows only the static deflection; the multi-point QS follows the oscillation at 1000 Hz

Legend: dynamic spring (blue), Claytex QS (red), multi-point QS (green).